Seismological and integrated geophysical research in Slovakia 2007-2010

Peter MOCZO[1,3], Miroslav BIELIK[2,3], Jozef KRISTEK[1,3], Miriam KRISTEKOVÁ[1,3], Martin GÁLIS[1,3], Lucia FOJTÍKOVÁ[3], Andrej CIPCIAR[1,3], Peter FRANEK[3], Erik BYSTRICKÝ[3]

[1] Department of Astronomy, Physics of the Earth and Meteorology, Division of Physics of the Earth, Faculty of Mathematics, Physics and Informatics, Comenius University, Mlynská dolina F1, 842 48 Bratislava, Slovak Republic; e-mail: moczo@fmph.uniba.sk

[2] Department of Applied and Environmental Geophysics, Faculty of Natural Sciences, Comenius University, Mlynská dolina, 842 15 Bratislava, Slovak Republic

[3] Geophysical Institute of the Slovak Academy of Sciences, Dúbravská cesta 9, 845 28 Bratislava, Slovak Republic

1. Numerical modeling of seismic motion and seismic wave propagation

A 3D hybrid finite-difference – finite-element viscoelastic modeling of seismic wave motion *(Galis et al., 2008)*

We have developed a new hybrid numerical method for 3D viscoelastic modeling of seismic wave propagation and earthquake motion in heterogeneous media. The method is based on a combination of the 4th-order velocity-stress staggered-grid finite-difference (FD) scheme that covers a major part of a computational domain, with the 2nd-order finite-element (FE) method which can be applied to one or several relatively small subdomains. The FD and FE parts causally communicate at each time level in the FD-FE transition zone. The transition zone consisting of the FE Dirichlet boundary, FD-FE averaging zone and FD Dirichlet zone is the key algorithmical part of the causally communicating FD and FE parts. Extensive numerical tests confirm that the smooth transition zone numerically performs better than the algorithmically minimal transition zone which does not include the FD-FE averaging zone.

The implemented FE formulation makes use of the concept of the global restoring-force vector which significantly reduces memory requirements com-

pared to the standard formulation based on the global stiffness matrix. The realistic attenuation in the whole medium is incorporated using the rheology of the generalized Maxwell body in definition by *Emmerich and Korn (1987)*. The rheology is strictly equivalent to that of the generalized Zener body - as shown by *Moczo and Kristek (2005)*.

The FE subdomains can comprise extended kinematic or dynamic models of the earthquake source or the free-surface topography. The kinematic source can be simulated using the body-force term in the equation of motion. The traction-at-split-node (TSN) method is implemented in the FE method for simulation of the spontaneous rupture propagation. The hybrid method can be applied to a variety of problems related to the numerical modeling of earthquake ground motion in structurally complex media and source dynamics.

The developed hybrid method can be applied to a variety of problems related to the numerical modeling of the earthquake ground motion in structurally complex media and particularly in near-surface laterally heterogeneous sedimentary structures including the free-surface topography and the extended kinematic or dynamic earthquake sources. The method can be also useful in the source dynamics studies.

Time-frequency misfit and goodness-of-fit criteria for quantitative comparison of time signals *(Kristekova et al., 2009)*

We elaborated and extended the concept of the time-frequency misfit criteria originally introduced by *Kristekova et al. (2006)*. *Kristekova et al. (2006)* used the time-frequency (TF) representation of signals to define envelope and phase differences at a point of the TF plane, and the corresponding TF envelope and phase misfit criteria. They defined and numerically tested globally normalized criteria for one-component signals assuming that one of the compared signals can be considered a reference. The locally normalized criteria were defined but not tested and analyzed.

The extension can be summarized as follows. We found more proper definition of the phase difference at a point of the TF plane. We defined TF misfit criteria for three-component signals. We distinguished two basic situations: 1. It is reasonable and possible to consider one of the compared signals a reference. 2. There is no reason, pertinent or attributable to the investigated problem, to choose one signal a reference. We also treated two principal normalizations of the misfits – local and global normalizations – in a unified way.

The values of the locally normalized misfit criteria for one point depend only on the characteristics at that point. The locally normalized misfit criteria should be used if it is important to investigate a) relatively small parts of the signal (e.g., wave groups, pulses, transients, spikes, so-called seismic phases), no matter how large amplitudes of those parts are with respect to the maximum amplitude of the signal, b) a detailed TF anatomy of the disagreement between signals in the entire considered TF region.

The globally normalized misfit criteria give the largest weights to the local envelope/phase differences for those parts of the reference signal (true or formally algorithmically determined) in which the envelope reaches the largest values. The globally normalized misfit criteria should be used if it is reasonable a) to quantify an overall level of disagreement, b) to account for both the envelope/phase difference at a point and the significance of the envelope at that point with respect to the maximum envelope of the reference signal, e.g., in the earthquake ground motion analyses and earthquake engineering.

We also introduced the TF envelope and phase goodness-of-fit criteria derived from the TF misfit criteria. Thus the TF goodness-of-fit criteria are based on the complete signal representation and have the same TF structure as the TF misfits. They are suitable for comparing arbitrary time signals in their entire TF complexity. The TF goodness-of-fit criteria quantify the level of agreement and are most suitable in the case of larger differences between the signals. They can be used when we look for the agreement rather than details of disagreement. The robust "verbal quantification" enables us to see/find out the "essential" level of agreement between the compared signals.

Program package TF_MISFIT_and_GOF_CRITERIA is available at http://www.nuquake.eu/Computer_Codes/.

A brief summary of some PML formulations and discretizations for the velocity-stress equation of seismic motion *(Kristek et al., 2009)*

The perfectly matched layer (PML) is an efficient tool to simulate nonreflecting boundary condition at boundaries of a grid in the finite-difference modeling of seismic wave propagation. We showed relations between different formulations of the perfectly matched layer with respect to their three key aspects – split/unsplit, classical/convolutional, with the general/special form of the stretching factor. We derived two variants of the split formulations for the general form of the stretching factor. Both variants naturally lead to the convolutional formulations in case of the general form of the stretching factor.

One of them, L-split, reduces to the well-known classical split formulation in case of the special form of the stretching factor. The other, R-split, remains convolutional even for the special form of the stretching factor. The R-split formulation eventually leads to the equations identical with those obtained straightforwardly in the unsplit formulation.

We also developed a time discretization of the unsplit formulation which is a slightly algorithmically simpler alternative to the time discretization presented by *Komatitsch and Martin (2007)*. The latter is shown in the form consistent with our discretization. We implemented both discretizations in the 3D velocity-stress staggered-grid finite-difference scheme. The interior grid was solved with the 4th-order whereas the PML with the 2nd-order scheme in space, both being the 2nd-order in time. Numerical tests showed a very good level of agreement of the two discretizations.

An adaptive smoothing algorithm in the TSN modelling of rupture propagation with the linear slip-weakening friction law *(Galis et al., 2010)*

We have developed an adaptive smoothing algorithm for reducing spurious high-frequency oscillations of the slip-rate time histories in the finite-element—traction-at-split-node modeling of dynamic rupture propagation on planar faults with the linear slip-weakening friction law. The algorithm spatially smoothes trial traction on the fault. The smoothed value of the trial traction at a grid point and time level is calculated if the slip is larger than 0 simultaneously at the grid point and 8 neighboring grid points on the fault. The smoothed value is a weighted average of the Gaussian-filtered and unfiltered values. The smoothed value of the trial traction at the grid point (i, j), at a given time level, is obtained as a weighted average of the Gaussian-filtered and unfiltered values:

$$\bar{\vec{T}}(i,j) = \sum_{k=1}^{3} \sum_{l=1}^{3} \bar{w}_{kl}\, \vec{T}(i+k-2, j+l-2) \ .$$

$\vec{T}$ denotes the original value of the trial traction,

$$\bar{w} = \begin{bmatrix} p/16 & p/8 & p/16 \\ p/8 & 1-3p/4 & p/8 \\ p/16 & p/8 & p/16 \end{bmatrix},$$

and parameter p varies during slip development linearly from 0 for zero slip

up to $p_{max} = 0.4$ for the critical slip value.

Extensive numerical tests demonstrate that the adaptive smoothing algorithm effectively reduces spurious high-frequency oscillations of the slip-rate time histories without affecting rupture time. The smoothing algorithm is a purely numerical tool. The algorithm does not need an artificial damping term in the equation of motion.

We implemented the smoothing algorithm in the finite-element part of the 3D hybrid finite-difference—finite-element method. This makes it possible to simulate dynamic rupture propagation inside a finite-element sub-domain surrounded by the finite-difference sub-domain covering major part of the whole computational domain.

We assume that the presented algorithm or some slightly modified algorithm should work also with the finite-difference implementations.

Quantitative comparison of four numerical predictions of 3D ground motion in the Grenoble Valley, France *(Chaljub et al., 2010)*

The third international symposium on the effects of surface geology in Grenoble, France, (ESG2006) provided an excellent opportunity to focus the traditional blind prediction experiment on numerical modeling of earthquake motion in a typical deep Alpine sediment-filled structure – the Grenoble valley.

Fourteen groups from 8 countries contributed to the ESG 2006 comparison with at least one numerical method and possibly different cases, providing a total of 18 prediction sets; seven groups addressed the 3D problem, out of which three could account for the effects of both underground and surface topography. The numerical schemes used for the 3D contributions belong to the finite-difference, spectral-element and discontinuous-Galerkin finite-element methods. Predictions by four participants were surprisingly close. They were analyzed and quantitatively compared using the misfit criteria proposed by *Kristekova et al. (2006)*.

One of the main lessons of this comparative exercise concerns the present capabilities of numerical simulation and is indeed a lesson of modesty: all the submitted predictions exhibit a very large variability. This variability confirms that the numerical prediction of ground motion in general certainly cannot be considered a mature, press-button approach, and the variability in direct uncorrected numerical predictions can be significantly larger than the variability associated with empirical predictions. This is also because not all applied numerical codes implement the best methodologically possible algorithms and

some of the codes are not yet bug free. Much care should be also given to an unambiguous definition of the "input solicitation" (input signal and/or source kinematics). Not sufficiently elaborated numerical predictions may yield wrong results and therefore will lead to large mistrust from end-users.

Another lesson: the striking similarity between predictions by completely different numerical methods is a very encouraging result. Despite the structural complexity, that is geometry and relatively large velocity contrast at the sediment-basement interface as well as smooth heterogeneity, and the methodological differences among the simulation methods, we found a surprisingly good level of agreement among four of the submitted predictions obtained by the finite-difference method (FDM), two implementations of the spectral-element method (SEM1 and SEM2) and arbitrary high-order derivative – discontinuous Galerkin method (ADER-DGM). It clearly shows that, when "used with caution", numerical simulation is actually able to handle correctly wave radiation from an extended source and their subsequent propagation in complex 3D media.

The comparison of the numerical predictions obtained with the FDM, two implementations of the SEM, and ADER-DGM indicates that each of these methods can be applied to simulation of the earthquake motion in structurally complex sediment-filled valleys with the flat free surface. In addition to being methodologically relatively simpler than the SEM and ADER-DGM, the presented implementation of the FDM can be computationally more efficient because the volume harmonic averaging of moduli and volume arithmetic averaging of density allows to account for irregular interfaces in regular grids well-suited to parallel implementation, while abrupt changes in the grid size are also allowed at the transition between sediments and much stiffer bedrock. In the case of the presented predictions, the FDM needed approximately 65% of the computational time used by SEM but, obviously, the difference may depend on the used computer and on the particular case under study. On the other hand, for the SEM and ADER-DGM the incorporation of the non-planar free-surface poses no methodological problem and thus the methods can be equally easily applied to both the flat and non-planar free surface.

Two main conclusions based on the ESG2006 simulation exercise and the detailed comparison of the four closest numerical predictions are:

1. No single numerical-modeling method can be considered as the best for all important medium-wavefield configurations in both computational efficiency and accuracy.

2. Reliable predictions of the earthquake ground motion in complex structures should be made using at least two different but comparably accurate methods to enhance reliability of the prediction. Our study indicates that the proper formulations and implementations of the FDM, SEM and ADER-DGM can be applied.

Local site-effects for the city of Thessaloniki (N. Greece) using a 3-D finite-difference method: a case of complex dependence on source and model parameters *(Skarlatoudis et al., 2010)*

The site effects of seismic motion in the metropolitan area of the city of Thessaloniki (Northern Greece) were investigated using a 3-D finite-difference modelling approach. Three different seismic scenarios were assumed with two different focal mechanisms for each one. Standard spectral ratios (SSR) were calculated from 3-D synthetics and compared with the ratios from the recorded motion, as well as ratios obtained from 1-D and 2-D modelling by other researchers. The average SSR curves from the six scenarios are in good agreement with the empirical ones. The SSR results from the 3-D modelling are different from those from the 1-D modelling, exhibiting higher fundamental frequencies and larger amplification amplitudes – in much better agreement with the observed SSR ratios. Comparisons of the Fourier amplitude spectra obtained for various scenarios for the broader area of Thessaloniki show considerable dependence of the site effects on the source properties (position, depth and fault-plane solution), as well as on the local structure.

On accuracy of the finite-difference and finite-element schemes with respect to P-wave to S-wave speed ratio *(Moczo et al., 2010)*

Numerical modeling of seismic motion in sedimentary basins often has to account for P-wave to S-wave speed ratios as large as five and even larger, mainly in sediments below groundwater level. Therefore, we analyzed finite-difference (FD) schemes

- displacement on a conventional grid (FD_D_CG),
- displacement-stress on a partly-staggered grid (FD_DS_PSG),
- displacement-stress on a staggered grid (FD_DS_SG),
- velocity-stress on a staggered grid (FD_VS_SG),

and the finite-element (FE) schemes,

- with Lobatto 4-point integration (FE_L),

- with Gauss 4-point integration (FE_G),
- with Gauss 1-point integration (FE_G1).

for their behavior with a varying P-wave to S-wave speed ratio.

We analyze 2D 2nd-order schemes assuming an elastic homogeneous isotropic medium and a uniform grid in order to compare schemes at the most fundamental level and identify basic aspects responsible for their behaviors with the varying speed ratio. We presented all the schemes in a unified form. We considered propagation of plane S wave and derived specific schemes.

We defined (full) local errors of the schemes in amplitude and polarization in one time step. Because different schemes use different time steps (following the appropriate stability conditions), we normalized the errors for a unit time. The normalization enabled us to directly compare errors of the investigated schemes.

Accuracy of the FD scheme on the conventional grid, FD_D_CG, strongly depends on the speed ratio. A computationally efficient application to sedimentary basins with a large speed ratio is practically impossible. Errors of the FD schemes on the staggered grid, FD_DS_SG and FD_VS_SG, are very close and small (in comparison to other schemes). The difference in errors is just due to different time-integrations in the schemes. The errors are practically insensitive to variation in the speed ratio. Considering the negligible difference between errors of FD_DS_SG and FD_VS_SG, schemes FD_D_CG and FD_DS_SG can be considered representative of the significantly different behaviors with varying speed ratio. The only apparent difference between the two schemes is in the way of approximating the second mixed spatial derivative. Where does it come from?

In deriving FD_DS_SG, only one and the same approximation formula is applied to all the first spatial derivatives. It is not so in FD_D_CG: one approximation formula is applied to the first spatial derivative in deriving the approximation to the second non-mixed derivative, whereas a different approximation formula is applied to the first spatial derivative in deriving the approximation to the second mixed derivative. The “heterogeneity” in approximating the first spatial derivatives seems to be the key factor causing the sensitivity of the scheme to varying and the inaccuracy of the scheme for large speed ratio.

Our results indicate that not only displacement FD schemes on the conventional grid but also displacement FE schemes on the conventional grid are inaccurate in media with a large P-wave to S-wave speed ratio if commonly

used spatial sampling is applied. FE_G1, identical with FD_DS_PSG, is an exception but (as it is well known) the scheme suffers from the presence of the hour-glass modes that have to be artificially suppressed.

Stable discontinuous staggered grid in the finite-difference modeling of seismic motion *(Kristek et al., 2010)*
We have developed an algorithm of the stable spatial discontinuous grid for the 3D 4th-order velocity-stress staggered-grid finite-difference modeling of seismic wave propagation and earthquake motion. The ratio between the grid spacings of the coarser and finer grids can be an arbitrary odd number. The stability of the algorithm is achieved by application of the Lanczos downsampling filter. The algorithm allows for large numbers of time levels without inaccuracy and possible eventual instability due to numerical noise that is generated at the contact of the two grids with different spatial grid spacings. The algorithm of the discontinuous grid is directly applicable also to the displacement-stress staggered-grid finite-difference scheme. The concept of the Lanczos downsampling filter is general and robust – its effect on the stability should not be dependent on a particular algorithm of the discontinuous grid.

2. Analysis of earthquakes and explosions

Focal mechanisms of micro-earthquakes in the Dobrá Voda seismoactive area and tectonic stress in the Malé Karpaty Mts (Little Carpathians), Slovakia *(Fojtíková et al., 2010; Briestenský et al., 2010)*
Focal mechanisms and moment tensor solutions for a set of weak earthquakes in the region of the Little Carpathians Mts. were determined. In order to account for small magnitudes of the analyzed earthquakes three independent methods were used for computation of the focal mechanisms. The majority of the analyzed micro-earthquakes have similar left-lateral strike-slip focal mechanism with weak normal or reverse components. Tectonic stress in the region of the Little Carpathians Mts. was estimated from stable focal mechanisms. The stress has a maximum compression in the northeast–southwest direction. The retrieved maximum compression lies along the belt of the Malé Karpaty Mts. Focal mechanisms of the selected earthquakes were confronted with the results of analyses of local measurements of microdisplacements at active tectonic faults.

Time-frequency analysis of explosions in the ammunition dismounting factory in Novaky, Slovakia *(Kristekova et al., 2008)*

A sequence of explosions occurred in the ammunition dismounting factory in Novaky, Slovakia, on March 2, 2007, and caused a major industrial accident in the history of Slovakia. Origin times and number of explosions were the key aspects for the state investigation team to explain primary cause and development of the accident. Analysis of seismic records was the only way to determine reliable origin times.

Only the strongest of the explosions Ex4 with Ml (BRA) = 2.1, was automatically located by the BRA, GFU and EMSC agencies. The automatic location by BRA used 8 automatic picks. Only 2 automatic picks available in the automatic system of BRA for explosion Ex3, with Ml (BRA) = 0.6, did not allow the automatic location. We can speculate that the threshold size of an event that can be automatically located by BRA lies somewhere in between Ex3 and Ex4, likely closer to Ex4.

Although the magnitude of Ex4 is close to the EMSC reporting threshold (2.0), the automatic locations of Ex4 by the BRA, GFU and EMSC agencies were sufficiently accurate – the distances between the true hypocenter and its automatic locations are at the level of round-off error.

The manual location made use of the identified phases (including S waves) from a larger number of stations and considerably improved the location – the distance between the true hypocenter and its location decreased from 5.7 km (automatic) down to 1 km (manual).

The time-frequency analysis (TFR) of the seismic records enabled us to identify specific TFR patterns that were afterwards interpreted as due to acoustic waves caused by two weaker explosions (Ex1 and Ex2) which we were originally unable to notice in the seismic records themselves due to the low signal to noise ratio and partial overlapping of the records. The TFR also led us to indication that the mechanism or conditions of Ex1 were different from those of other explosions, mainly Ex3 and Ex4. Ex1 produced relatively stronger acoustic wave. Moreover, the detailed TFR led to indication of two another weaker explosions with timing between Ex1 and Ex2.

Our results are supported by the on-site investigations based on the directly found and uncovered craters, distribution of explosives, and the other available facts. Ex1 was the first initialization explosion. The crater was found after removal of debris. The conditions and type of explosives were different from those in the later explosions. Ex1, inside a building, had caused a fire which

then spread through halls and corridors and initiated later explosions of the explosives stored at different sites. The sites of craters and estimated scenario are consistent with timing found by our analysis of seismic records. The state investigation team also admitted the two indicated weakest explosions based on the distribution of explosives.

This case study indicates that the time-frequency analysis can considerably help in interpretation of seismic records and identification of explosions. In this case the determined hypocentral times of the explosions are the only reliable times the state investigation team could use.

3. The monitoring of earthquakes

Networks of seismic stations

The Geophysical Institute of Slovak Academy of Sciences (GPI SAS) operates the National Network of Seismic Stations (NNSS), and analyzes instrumental and macroseismic data for earthquakes from territory of Slovakia. The seismic stations of NSSS are deployed with the intention to determine seismic source zones on the Slovak territory more precisely and to allow to record and localize any earthquake with possible macroseismic effects and with epicenter on the Slovak territory. Map with locations of the NNSS seismic stations is shown in Fig. 1.

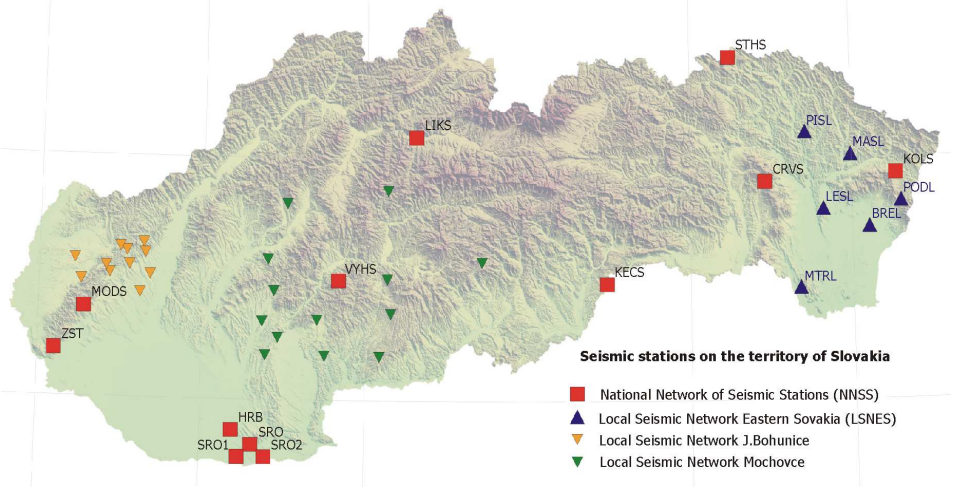

Fig. 1. The seismic stations on the territory of Slovakia.

Faculty of Mathematics, Physics and Informatics of Comenius University in Bratislava (FMPI UK) operates the Local Seismic Network Eastern Slovakia (LSNES) and analyzes instrumental data for the eastern part of Slovakia. The seismic stations of LSNES are deployed with intention to better monitor and understand the seismic regime of that part of our territory. The decision about importance of more detailed monitoring of seismic activity in eastern Slovakia by local seismic network was accepted by the Slovak Government after the wide-felt earthquake in Jasenovo on May 20, 2003 (M_L = 3.7, I_0 = 6-7). Thereafter the LSNES was planned, constructed and finally put in operation in 2007. Locations of the LSNES seismic stations are shown in Fig. 1.

Besides the two seismic networks operated by research institutions, there are two local seismic networks on the territory of Slovakia operated by company Progseis, s.r.o. Seismic stations of these networks are deployed around two nuclear power plants Jaslovské Bohunine and Mochovce (Fig. 1) with intension to monitor in detail local seismic microactivity.

Data collection, processing and analysis

A data centers of the national network and of the local network Eastern Slovakia are located in the GPI SAS, Bratislava or in the FMPI UK, Bratislava, respectively. Both data centers are created in the mirror way, equipped with the similar software and functional features. The data center collects waveforms from all stations of NNSS and LSNES and from selected seismic stations of some other institutions from Central and Southeastern European countries. Data are collected in real or near-real time using the SeisComp/SeedLink *(Hanka et al., 2000; Van Eck et al., 2004; Hanka and Saul, 2006)* or SEMS SeedLink software, respectively. The miniSeed format is used for both data collection and data exchange. In total, data from 62 seismic stations are collected. These stations create Regional Virtual Seismic Network in the GPI SAS (Fig. 2). More information about NNSS and live seismograms from the seismic stations of NNSS are available at http://ww.seismology.sk web page. Live seismograms are archived for 30 days. More information about LSNES can be found at http://www.fyzikazeme.sk /mainpage/index_en.htm.

Seismic waveforms are exchanged with all institutions which supply data to the data center in Bratislava. In addition, the seismic waveforms are sent also to the Orfeus Data Center, De Bilt, Netherlands.

A two-step analysis of seismic waveforms is performed – automatic analysis and localization of earthquakes and manual analysis and localization.

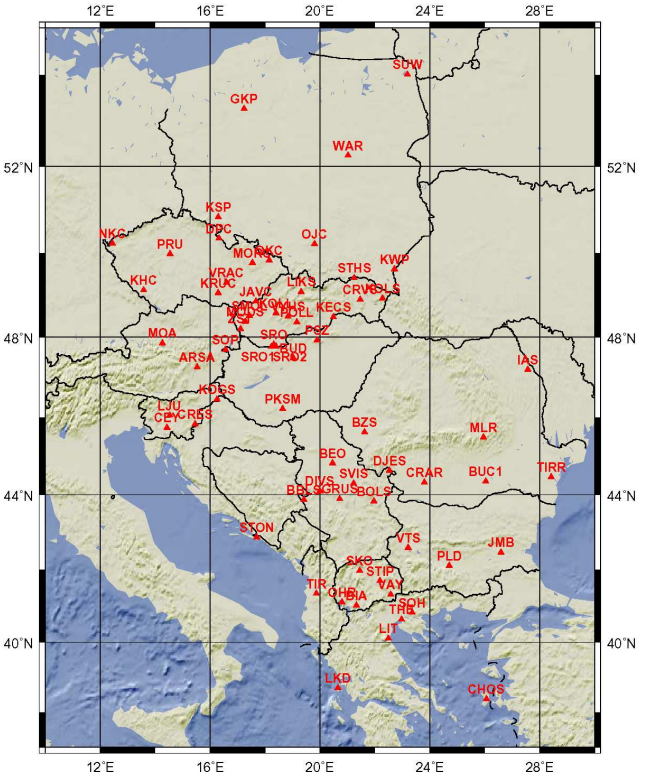

Fig. 2. Virtual Regional Seismic Network in the Geophysical Institute, Slovak Academy of Sciences, Bratislava.

The automatic analysis is performed in real time by AutoLoc package of GFZ Potsdam *(Hanka and Saul, 2006)*. If the alert criteria are met, information is sent to the Civil Protection and other relevant authorities. Automatic locations are also sent to international data center CSEM-EMSC.

The manual analysis is performed on daily basis using the Seismic Handler package since October 2003 *(Stammler, 1993)*. The results of waveform interpretation and earthquake localization are stored in a database which is in operation since 1996. Fig. 3 shows an example of an event interpretation for the April 30, 2011, M_L=2.8 mining event from the Lubin area, Poland.

Besides seismometric data, the GPI SAS collects and analyzes macroseismic data. In case of an earthquake with possible macroseismic effects on the

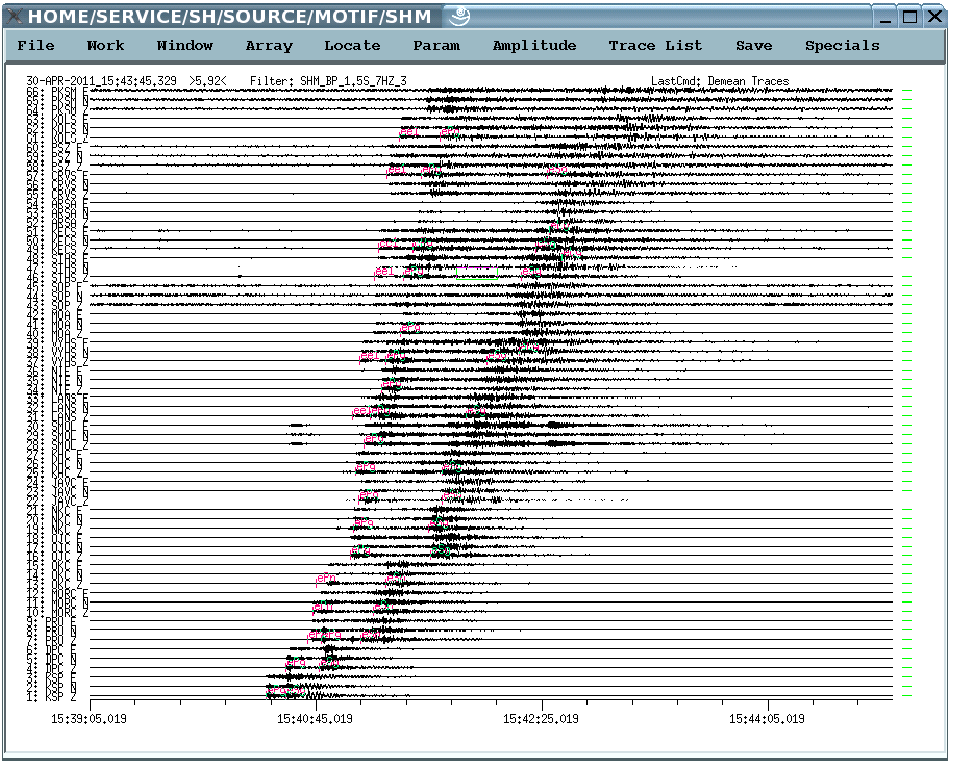

Fig. 3. An example of manual event interpretation using the Seismic Handler package. Displayed traces are from the Virtual Regional Seismic Network in the GPI SAS Bratislava for the April 30, 2011, ML=2.8 mining event in the Lubin area, Poland.

territory of Slovakia, the GPI SAS issues public information and request for people to contact the institute if they observed macroseismic effects of the earthquake. Then macroseismic questionnaires are sent to people or people can download them from the http://www.seismology.sk web page. If there is a possibility of exceeding intensity 6º EMS-98 in some localities, an on-site macroseismic survey is performed. Macroseismic intensity is then estimated for each locality using available macroseismic observations. The macroseismic intensity is estimated in degrees of a macroseismic scale EMS 98 *(Grünthal, ed. 1998).*

Seismic activity on the territory of Slovakia in the period 2007-2010

The seismic activity on the territory of Slovakia for the period 2007-2010 is briefly characterized in Table 1 and illustrated in Fig. 4a, 4b.

Using data from the seismic stations of NNSS and LSSVS, 235 local earthquakes without macroseismic observations (microearthquakes) were localized with epicenter on the territory of Slovakia and in border areas in the years 2007-2009. Seismic activity for year 2010 is in the process of final reinterpretation and we can assume about 90 localized microearthquakes with epicenter on the territory of Slovakia and in border areas. Microearthquakes occurred in all known Slovak seismic source zones. The most active during the reported period 2007-2010 seems to be the eastern part of Slovakia. The local seismic network LSNES contributed to the knowledge of this activity considerably. For instance, in the beginning of 2009 (in the span of 3 weeks) occurred a sequence of approximately 30 earthquakes with epicenters in Slovak-Ukraine border area – 3 of them with reported macroseismic observations. In most cases, it would be impossible to perform seismometric localization of epicenter of earthquakes from the eastern sequence without data from the seismic stations of LSNES.

Table 1. Seismic activity on the territory of Slovakia in the period 2007-2010

Year	Microearthquakes	Macroseismically observed earthquakes (epicenter in SK)	Macroseismically observed earthquakes (epicenter outside SK)
2007	72	0	0
2008	81	3	0
2009	82	5	1
2010	cca 90	3	0

During the period 2007-2010, 12 earthquakes were macroseismically observed on the territory of Slovakia. Expect for one earthquake in the Central Slovakia, macroseismically observed earthquake occurred in the eastern part of Slovakia. One earthquake with epicenter in Austria was macroseismically observed on the territory of Slovakia too. Epicenter of this earthquake is not

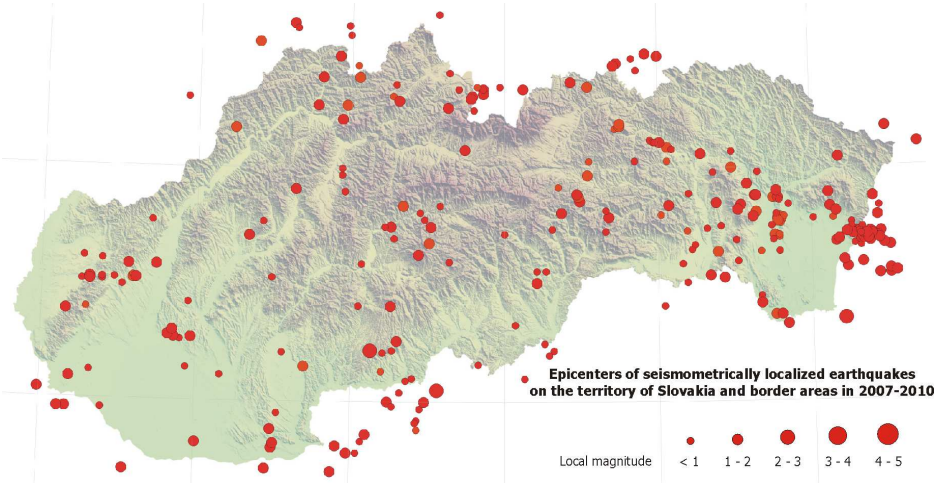

Fig. 4a. Epicenters of seismometrically localized earthquakes on the territory of Slovakia and border areas in 2007-2010. (Only preliminary results for January-July 2010 are shown).

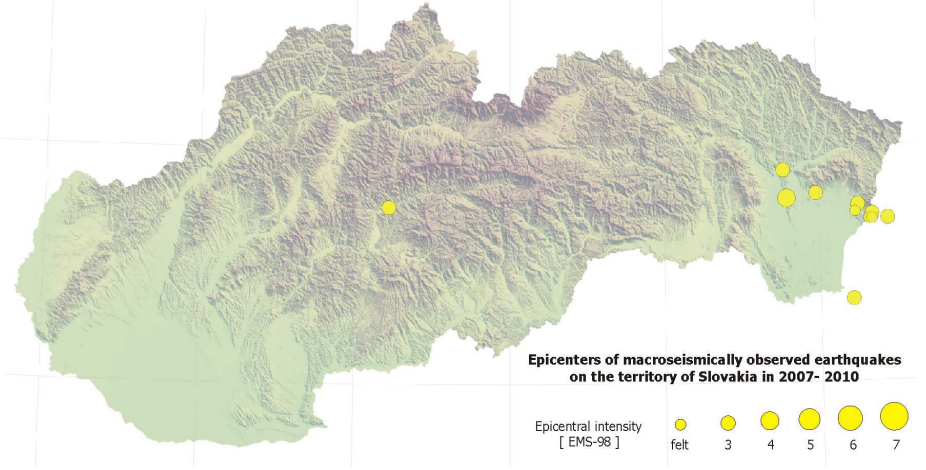

Fig. 4b. Epicenters of macroseismically observed earthquakes on the territory of Slovakia in 2007-2010.

depicted in the Fig. 4b because its location is outside of the region displayed in the figure. The highest reported macroseismic intensity was 4° EMS 98 for the earthquake with epicenter in the Eastern Slovakia (4. 4. 2010). This earthquake

was felt in 12 localities in the Eastern Slovakia. The question remains how to estimate the extent and intensity of the macroseismic observations of 3 earthquakes from the sequence in the Eastern Slovakia in the beginning of 2009 that were reported to be macroseismically observed. Despite the fact that more than 100 macroseismic questionnaires were requested and sent to people, only 2 of them returned back.

Export of know-how in seismic monitoring within the framework of the official Slovak Development Aid SlovakAid

Slovak seismologists exported their experiences and know-how and helped to build modern seismic monitoring systems in countries of seismically active Balkan region within several projects of the official Slovak Development Aid. The two projects in period 2007-2010 were preceded by other Slovak development aid projects aimed on building new and modernization of existing seismic monitoring infrastructure in Serbia (project Development of Infrastructure for Rapid Earthquake Data Collection and Exchange DIRECTE 2004-2005) and in Macedonia (Development of Infrastructure for Rapid Earthquake Data Collection and Exchange – part2 DIRECTE2 2004-2005).

The project ShareDIRECTE (Sharing the Data from the Infrastructure for Rapid Earthquake Data Collection and Exchange 2006-2008) was a natural continuation of the previous project DIRECTE. Its goal was to apply the results of the DIRECTE project in practice and to share the obtained seismic information with governmental authorities as well as with the public and to contribute to the better preparedness of the country to strong earthquake. Thanks to the results of both these projects the Civil Protection in Serbia will be able better and more efficiently react to the emergency situations caused by strong earthquake.

The project DETERMINE (Development of Earthquake Monitoring Infrastructure for Bosnia and Herzegovina, November 2009 – February 2011) was a response to the urgent need of the state-of-the-art seismic monitoring system on the territory of Bosnia and Herzegovina. The seismic monitoring systems consisting from four seismic stations and data center were delivered to and installed in each of both entities of Bosnia and Herzegovina. The real-time continuous data acquisition from the installed seismic stations and the international real-time data exchange were established in the framework of the project. The important part of the project was education of the experts from Bosnia and Herzegovina in the field of seismic monitoring.

4. Carpathian-Pannonian lithosphere: integrated geophysical study

Solution of 3D forward gravimetric problem in the Western Carpathian-Pannonian region

Alasonati Tašárová et al. (2008, 2009) presented the first three-dimensional (3D) combined gravity and seismic modeling in the Western Carpathian-Pannonian region, based mainly on the CELEBRATION 2000 data *(e.g. Środa et al., 2006; Grad et al., 2006)*. The forward modeling of the Bouguer gravity anomaly was performed using the Interactive Gravity and Magnetic System (IGMAS) *(e.g. Götze, 1976; Götze and Lahmeyer, 1988)*. The modeled geological bodies are in IGMAS approximated by polyhedra of constant density. The structures are defined and modeled along 2D cross-sections that are automatically connected via triangulation into a volume. Thus, the geometry of the geological bodies between the cross-sections is interpolated. Therefore, in order to obtain more reliable results, a greater number of 2D planes must be included. The model presented was developed along 36 cross-sections, separated by 10 to 20 km across the Western Carpathians and Pannonian Basin (the focus of the modeling) and 40 km in the surrounding Bohemian Massif and Eastern Alps. The model reaches the depth of 250 km. The direction of the modeled cross-sections is identical to one of the seismic profiles from the CELEBRATION 2000 experiment (CEL05 profile).

Constraining data and density determination. Seven CELEBRATION 2000 profiles were used for the combined 3D gravity-seismic modeling: CEL01, CEL02, CEL03, CEL04, CEL05, CEL09 and CEL 10 *(Środa et al., 2006; Malinowksi et al., 2005; Janik et al., 2005; Grad et al., 2006; Hrubcová et al., 2005, 2008)*. Moreover, the results from 2D integrated modeling of *Zeyen et al. (2002)* and *Dérerová et al. (2006)* served as a starting point for the 3D gravity modeling. First of all, these results constrained one of the two input parameters used for the gravity modeling, namely the geometry of the modeled structures (i.e. depth to the main boundaries). The density, which is the second input parameter, can be constrained by geological data. The results from borehole measurements provide the best information on the composition of the rocks. However, such measurements are only sparse and restricted to the uppermost part of the upper crust. At larger depths and for large-scales models, other information constraining the composition must be used. For the igneous rocks, relationships of *Christensen and Mooney (1995)* and *Sobolev and Babeyko (1994)* were applied. Since the tectonic units of the modeled region are

characterized by extremely different thermal regimes, the relationship of *Sobolev and Babeyko (1994)* was found more appropriate for the density determination. The densities of the sediments in the units surrounding the Western Carpathian-Pannonian region were calculated from the P-wave seismic velocities using the relationships of *Gardner et al. (1974)* and *Wang (2000)*. The densities of the sediments in the Pannonian Basin (PB) and Western Carpathians were based on the previous investigations *(e.g. Makarenko et al., 2002; Bielik et al., 2005)*. Nevertheless, both densities and geometries were subject of the modeling and the resulting values are a trade-off between the seismic results and gravity anomalies.

The temperature and density distribution in the uppermost mantle was calculated using a combination of petrological, mineralogical and geophysical information. This calculation was performed in order to enhance the 3D gravity modeling, particularly in the PB, because it is characterized by an asthenospheric upwelling and thus by anomalous temperatures and densities in the uppermost mantle. The mantle densities were estimated using the methodology of *Afonso (2006)*. This approach is based on a self-consistent combination of data from petrology, geophysics, mineral physics and thermodynamics. The numerical implementation of this method, referred to as LitMod, is a 2D code. Based on the input parameters (thermal conductivity, radiogenic heat production, crustal densities, chemical composition of the uppermost mantle), it calculates temperature and pressure distribution within the whole lithosphere and sublithospheric mantle, and for the mantle part also densities and seismic velocities. The calculations were performed along 3 selected profiles and the resulting structures were extrapolated into the 3D gravity model *(Alasonati Tašárová et al., 2009)*.

Results. The thickness of the sediments in the different sedimentary units is quite variable. In the PB in it reaches 0–7.8 km. The Western Carpathians are characterized by infill of 0–2 km in the Inner Western Carpathians, maximum of 21.5 km in the Outer Western Carpathians flysch zone and 1–3 km in the Western Carpathian Foredeep. Note that the maximal value of 21.5 km includes both the sediments of the Outer Western Carpathian Flysch zone and the Trans European Suture Zone (TESZ) cover, which contains the Upper Palaeozoic to Mesozoic strata (Środa et al., 2006). The southern part of the Polish Basin, which was included in the 3D model, has sedimentary infill of ~7 km. The border between the TESZ and the East European Craton (EEC – Lublin

Trough) is characterized by 5 to 8 km of sedimentary cover. Elsewhere, the EEC is covered by a thin layer of sediments (less than 3 km).

The thinnest crust was modeled in the central and eastern part of the PB. The minimum crustal thickness of ~22 km is located along the CEL05. The Danube Basin is characterized by crustal thickness of 28–30 km, increasing to 35 km toward the west. The Central Western Carpathians have 28–35 km thick crust, while the crust beneath the Outer Western Carpathians and the Carpathian Foredeep is 35 to 43 km thick. The maximum crustal thickness of ~50 km is modeled beneath the TESZ/EEC along the CEL05.

Similarly to the crust, also the lithospheric mantle resulting from our best-fitting model is extremely thin in the PB. The lithosphere-asthenosphere boundary (LAB) reaches here depths of 60–100 km. The lithospheric thickness is gradually increasing toward the west and north. In general, the lithosphere is ~160 km thick in the Eastern Alps, ~140 km in the Bohemian Massif and Western Carpathians. The thickest lithosphere (~200 km) is included in the EEC.

The 3D model enabled also to perform gravity stripping. It allowed to identify the sources of the anomalies, to separate their effects and localize the lithospheric inhomogeneities. The sediment stripped map of the PB is generally characterized by a positive anomaly of 20–50 mGal. Particularly the eastern part of the PB is characterized by pronounced residual gravity high, which is related to the extremely shallow Moho in this region. In contrary, the Central Western Carpathians reflects a negative effect of the thick low-density upper and middle crust. The thickness of the upper and middle crust reaches in the density model 25 km. A complete stripped map was calculated by removing the gravity effects of the sediments, Moho and the low-density uppermost part of the upwelling asthenosphere from the Bouguer anomaly. In contrast to the sediment stripped map, it clearly shows similarities of the PBS and Western Carpathians. The Moho in the PB is some 10 km shallower than in the Western Carpathians. When its gravity effect is accounted for (together with the low-density upwelling asthenosphere in the PBS), both microplates ALCAPA and Tisza-Dacia are characterized by residual anomalies, which are much lower than in the surrounding regions. The greatest gradient coincides with the location of the PKB, separating the microplate ALCAPA from the platform. This suggests that the lithospheric structure of the microplates ALCAPA and Tisza-Dacia is in terms of density distribution quite different from the surrounding units. Also, it can be reflecting different degree of crustal con-

solidation. It follows that the ALCAPA and Tisza-Dacia are characterized by low-density unconsolidated crust, whereas the European Platform has a consolidated crust of high-densities.

Solution of 3D forward gravimetric problem in the Liptovská kotlina basin region

Detailed 3D forward gravity modelling was applied for calculation of the stripped gravity map in the Liptovská kotlina basin (*Szalaiová et al., 2008*). The Liptovská kotlina basin is located in the northern part of Slovakia, just at the bottom of the High Tatras. This territory orthographically represents an extensive terrain depression of an irregular shape, elongated in the east-west direction. The length and width of the Liptovská kotlina basin are 50 km and 15 km, respectively. It slopes from the east to the west with the average elevation difference of 550 m. It is built by the Quaternary and Central Carpathian Palaeogene sediments. The Palaeogene filling of the basin represents one of the most classic developments of the Central Carpathian Palaeogene. A number of mineral and thermal water springs is located in the Liptov region. The growing interest for the use of geothermal water for energetic purposes and recreation in an attractive territory makes the Liptovská kotlina basin a very interesting locality. It is well-known that Mesozoic rocks in the basement are possible thermal water collectors. From this point of view a research concerning the structure of the pre-Tertiary basement is very important.

It is well-known that for an objective study of the basement structure it is very useful to calculate the stripped gravity map. Therefore the paper focused on the calculation of the stripped gravity map in the Liptovská kotlina basin by means of 3D forward gravity modeling. The stripped gravity map is a result of subtracting the 3D gravity effect of the sedimentary filling density contrast from the Bouguer gravity anomalies. This type of gravity map contributes significantly to the geophysical investigation of the basement structures in the Liptovská kotlina basin and to an assessment of assumed geothermal water supply.

The resultant stripped gravity maps showed new gravity features, which consist of the relative gravity highs and lows. The largest gravity high correlates with the cropping out of the Tatricum on the northern margin of the Liptovská kotlina basin. The source of this anomaly would be looked for in the larger mass of the crystalline rocks underlying the cover unit, as well as the Fatricum and Hronicum tectonic units. A significant gravity high can be seen in

the Liptovská Mara depression. It consists of two local maxima. The first maximum is probably due to the rocks of the Hronicum with higher density (predominantly dolomites), while the second maximum could result in the rocks of the Fatricum which are underlain by Tatricum. The source of the Štrbské Pleso gravity high can be explained by the elevation of the Tatricum underlain by Mesozoic rocks. The Štrba gravity high can be explained by higher density masses of volcano-sedimentary Palaeozoic rocks of the Hronicum complex. The pattern of the gravity field on the stripped gravity map is also accompanied by the gravity lows. They are characterized by almost the same amplitude values of –62 mGal. One can be observed in the west-eastern part of the Liptovská kotlina basin. This gravity low, consisting of two different local minima, is due to less dense marly rocks of the Hronicum. The same source is also suggested for the gravity lows extended in the southernmost part of the Liptovská kotlina basin. Note that the depressions of the Fatricum unit in the basement of the Hronicum could also represent a partial source of all the relative gravity lows.

2D gravity field interpretation in the Turčianska Kotlina Basin

Grinč et al. (2010) studied the geological structure and composition of the Turčianska Kotlina Basin by the quantitative interpretation of the gravity field. The interpretation was done by application of the 2D density modeling method using the GM-SYS software. Geophysical constraints of the density models were represented by the existing geophysical measurements and interpretations. The Tučianska Kotlina Basin in the picture of the regional gravity field is characterized by the local gravity low with amplitude of about 12 mGal. The source of this gravity low is low density Tertiary sediments, which fill the basin. From the Tertiary sediments the Neogene sediments play dominant role in observed gravity, because their gravity effects are considerably larger in comparison with the gravity effects of the Paleogene sediments. The contacts between the Malá Fatra and Veľká Fatra Mts., and the Turčianska Kotlina Basin are characterized by the significant gravity gradients. They reflect tectonic contact between the basin and crystalline core mountains. In the Turčianska gravity low we can see three local gravity lows. The highest local gravity low is explained by the largest thickness of the Tertiary sediments. Another two local gravity lows are also characterised by thicker layers of the Tertiary sediments. Density models assume that the eastern (western) part of the basin basement is built by the Mesozoic (crystalline) rocks. In the central

part of basin the thick Paleogene sedimentary filling (more than 1 km) compensates the deepest part of the pre-Tertiary basement. 2D density models in the basin do not suggest a presence of the Paleogene sediments in the eastern part of the basin filling. It is also indicated that the Mesozoic rocks underlie the Tertiary sediments. The pre-Tertiary basement was interpreted in the depths from 0 km up to the 2 km. Note that all geological structures (blocks) are sliding from the East to the West. The dipping of the Malá Fatra Mts. is steeper than in a case of the Veľká Fatra Mts. The anomalous bodies observed on the western part of the basin result from the alluvial and detrital cones. Their presence and gravity effect can be observed mainly on the eastern slope of the Malá Fatra Mts.

Modeling refracted and reflected waves along the CELEBRATION 2000 profiles

During the CELEBRATION 2000 seismic experiment, the Western Carpathians and Pannonian basin region was investigated by a dense system of deep seismic sounding profiles. In the paper of *Grad et al. (2007)* it was presented the results of modeling refracted and reflected waves employing 2-D ray tracing for seven interlocking profiles CEL01, CEL04, CEL05, CEL06, CEL11, CEL12 and CEL28, that were jointly modeled and interpreted with the constraint that the models match at the crossing points of the profiles. The resulting P-wave velocity models revealed complex structures in the crust and large variations in the depth of the Moho discontinuity (~25-45 km). In the southern part of the area, the relatively thin Pannonian basin crust consists of 3-7 km thick sediments and two crustal layers with velocities of 5.9-6.3 km/s in the upper crust and 6.3-6.6 km/s in the lower crust. In the central region, the upper crust of the ALCAPA (Alpine-Carpathian-Pannonian) microplate contains a high velocity body of $V_p \geq 6.4$ km/s, which spatially corresponds with the Bükk Composite Terrane. The total thickness of the ALCAPA crust is 1-2 km greater than in the adjacent Tisza-Dacia microplate. To the north in the area of the TESZ and Carpathian foredeep, it was observed a 10-20 km thick upper crust with low velocity ($Vp \leq 6.0$ km/s). Sub-Moho velocities have average values of 7.8-8.0 km/s for the Pannonian basin, while in the Western Carpathians, the TESZ and the East European Craton (EEC) area, they are slightly higher (8.0-8.1 km/s). Lower velocities beneath the ALCAPA and Tisza-Dacia microplates could be caused by compositional variations and the significantly higher surface heat flow. Beneath some profiles, reflectors in the lithospheric mantle

were found sub-parallel to the Moho but 10-20 km below it. Our integrated geophysical and geological analysis indicates that the observed structure was created by collision of two lithospheric plates with only a moderate degree of convergence. The northern plate consists of older European tectonic units of the EEC and TESZ. However, the southern one consists of younger tectonic units of the Western Carpathians and the back-arc Pannonian basin that generated the ALCAPA and Tisza-Dacia microplates. The authors interpreted the complex present day structure to be the result of the soft continental collision between the ALCAPA and Tisza-Dacia microplates and the south margin of the European plate, which was mainly followed by the extensional process beneath the back-arc Pannonian basin.

Interpretation of deep seismic reflection profiles in the northern part of the Malé Karpaty Mountains

Interpretation of deep seismic reflection profiles in the northern part of the Malé Karpaty Mountains, which are westernmost part of the Western Carpathians was presented in the paper published by *Kytková et al. (2007)*. The goal was to recognize the tectonic character of western and eastern mountain range limitation in the area between Plavecký Mikuláš and Dolné Orešany, study the character of the Záhorsky fault and the declination of inner structures. Result of the interpretation was the confirmation that the Vienna Basin is a pull-appart basin and that the western mountain range border is formed by an orthogonal strike slip connected with the mountain range uplift. On the eastern border (from the Danube Basin side) which was until now considered as fault, appears to have a fold character. Hence, the Malé Karpaty Mountains represent at least in the northern part an anticline.

The improved geophysical image of the lithospheric structure and tectonics in the Carpathian-Pannonian Basin region, which was based on our systematic and integrated intepretation of the geophysical fields was presented and summerized in the papers of *Bielik et al. (2010); Bielik et al. (2009); Vozár et al. (2007)* and *Plašienka et al. (2008)*. The method of the 2-D integrated geophysical modelling was also applied in study of the lithosphere in Aswan area *(Radwan et al., 2007)*.

References

Afonso J. C., 2006: Thermal, density, seismological, and rheological structure of the

lithospheric-sublithospheric mantle from combined petrological-geophysical modeling: Insights on lithospheric stability and the initiation of subduction. Ph.D. thesis, Carleton Univ., Ottawa.

Bielik M., Makarenko I., Starostenko V., Legostaeva O., Dérerová J., Šefara J., Pašteka R., 2005: New 3D gravity modeling in the Carpathian-Pannonian region. Contrib. Geophys. Geod., **35**, 1, 65–78.

Christensen N. I., Mooney W. D., 1995: Seismic velocity structure and composition of the continental crust: A global view. J. Geophys. Res., **100**, B7, 9761–9788.

Dérerová J., Zeyen H., Bielik M., Salman K., 2006: Application of integrated geophysical modeling for determination of the continental lithospheric thermal structure in the eastern Carpathians. Tectonics, **25**, TC3009, doi: 10.1029/2005TC001883.

Emmerich H., Korn M., 1987: Incorporation of attenuation into time-domain computations of seismic wave fields. Geophysics, **52**, 1252–1264.

Gardner G. H. F., Gardner L. W., Gregory A. R., 1974: Formation velocity and density – The diagnostic basics for stratigraphic traps. Geophysics, **29**, 6, 770–778.

Götze H.-J., Lahmeyer B., 1988: Application of three-dimensional interactive modeling in gravity and magnetics. Geophysics, **53**, 8, 1096–1108.

Götze H.-J., 1976: Ein numerisches Verfahren zur Berechnung der gravimetrischen und magnetischen Feldgrößen für dreidimensionale Modellkörper. Dissertation, Technical University Clausthal, Germany.

Grad M., Guterch A., Keller G. R, Janik T., Hegedus E., Vozar J., Slaczka A., Tiira T., Yliniemi J., 2006: Lithospheric structure beneath trans-Carpathian transect from Precambrian platform to Pannonian basin: CELEBRATION 2000 seismic profile CEL05. J. Geophys. Res., **111**, B03301.

Grünthal G. (Eds.), 1998: European Macroseismic Scale 1998. Conseil de l`Europe, Cahiers du Centre Européen de Géodynamique et de Séismologie, Luxembourg, **15**, 99 p.

Hanka W., Heinloo A., Jäckel K.-H., 2000: Networked Seismographs: GEOFON Real-Time Data Distribution, ORFEUS Electronic Newsletter, **2**, 3. (http://orfeus. knmi.nl/)

Hanka W., Saul J., 2006: GEOFON and its Role in Earthquake Monitoring and Tsunami Warning. Proceedings of the NATO Workshop on Earthquake Monitoring and Seismic Hazard Mitigation in Balkan Countries, Borovetz, Bulgaria, September 11-17, 2005.

Hrubcová P., Środa P., Špičák A., Guterch A., Grad M., Keller G. R., Brückl E., Thybo H., 2005: Crustal and uppermost mantle structure of the Bohemian Massif based on CELEBRATION 2000 data. J. Geophys. Res., **110**, B11305.

Hrubcová P., Środa P., CELEBRATION 2000 Working Group, 2008: Crustal structure at the easternmost termination of the Variscan belt based on CELEBRATION 2000 and ALP 2002 data. doi: 10.1016/j.tecto.2008.07.009, Tectonophysics, **460**, 55–75.

Janik T., Grad M., Guterch A., Dadlez R., Yliniemi J., Tiira T., Keller G. E., Gaczyński G. R., CELEBRATION 2000 Working Group, 2005: Lithospheric structure of the Trans-European Suture Zone along the TTZ-CEL03 seismic transect (from NW to SE Poland). Tectonophysics, **411**, 129–156.

Komatitsch D., Martin R., 2007: An unsplit convolutional Perfectly Matched Layer improved at grazing incidence for the seismic wave equation. Geophysics, **72**, SM155–SM167.

Kristeková M., Kristek J., Moczo P., Day S. M., 2006: Misfit Criteria for Quantitative Comparison of Seismograms. Bull. Seism. Soc. Am., **96**, 1836–1850.

Makarenko I., Legostaeva O., Bielik M., Starostenko V., Dérerová J., Šefara J., 2002: 3D gravity effects of the sedimentary complexes in the Carpathian-Pannonian region. Geologica Carpathica, **53**, Special Issue.

Malinowski M., Zelazniewicz A., Grad M., Guterch A., Janik T., 2005: Seismic and geological structure of the crust in the transition from Baltica to Palaeozoic Europe in SE Poland - CELEBRATION 2000 experiment, profile CEL02. Tectonophysics, **401**, 1-2, 55–77.

Moczo P., Kristek J., 2005: On the rheological models used for time-domain methods of seismic wave propagation. Geophys. Res. Lett., **32**, L01306.

Sobolev S. V., Babeyko A. Y., 1994: Modeling of mineralogical composition, density and elastic wave velocities in anhydrous magmatic rocks. Surveys in Geophysics, **15**, 5, 515–544.

Stammler K., 1993: Seismic-Handler - Programmable multichannel data handler for interactive and automatic processing of seismological analyses. Computers & Geosciences, **19**, 2, 135–140.

Środa P., Czuba W., Grad M., Guterch A., Tokarski A. K., Janik T., Rauch M., Keller G. R., Hegedüs E., Vozar J., Celebration 2000 Working Group, 2006: Crustal and upper mantle structure of the Western Carpathians from CELEBRATION 2000 profiles CEL01 and CEL04: seismic models and geological implications. Geophys. J. Int., **167**, 737–760.

Van Eck T., Trabant C., Dost B., Hanka W., Giardini D., 2004: Setting up a virtual Broadband Seismograph Network Across Europe. EOS, Transactions, AGU, **85**, 13, 125–129.

Wang Z., 2000: Velocity-Density Relationships in Sedimentary Rocks. Geophysics reprint series, **19**, 258–268, Society of Exploration Geophysicists.

Zeyen H., Dérerová J., Bielik M., 2002: Determination of the continental lithosphere thermal structure in the western Carpathians: Integrated modeling of surface heat flow, gravity anomalies and topography. Phys. Earth Planet. Inter., **134**, 89–104.

Publications

Alasonati Tašárová Z., Bielik M., Götze H. J., 2008: Stripped image of the gravity field of the Carpathian-Pannonian region based on the combined interpretation of the CELEBRATION 2000 data. Geologica Carpathica, **59**, 3, 199–209.

Alasonati Tašárová Z., Afonso J. C., Bielik M., Götze H. J., Hók J., 2009: The lithospheric structure of the Western Carpathian-Pannonian Basin region based on the CELEBRATION 2000 seismic experiment and gravity modeling. Tectonophysics, **475**, 3-4, 454–469.

Archuleta R. J., Moczo P., Labák P. (Eds.), 2007: Proceedings of the Workshop - Abstract Book. Numerical Modeling of Earthquake Source Dynamics - NMESD 2007. FMFI UK a GFÚ SAV, Bratislava. 54 p.

Archuleta R. J., Moczo P., Kristek J., Galis M. (Eds.), 2010: Proceedings of the Workshop - Abstract Book. Earthquake Source Dynamics: Data and Data-constrained Numerical Modeling - ESD 2010. FMFI UK a GFÚ SAV, Bratislava, 69 p.

Bielik M., Šefara J., Alasonati Tašárová Z., Vozár J., 2009: Geofyzikálny obraz karpatsko-panónskej oblasti. In: Spoločný geologický kongres Českej a Slovenskej geologickej spoločnosti. Bratislava, Štátny geologický ústav D. Štúra, 1–20. ISBN 978-80-89343-24-9.

Bielik M., Alasonati Tašárová Z., Zeyen H., Dérerová J., Afonso J. C., Csicsay K., 2010: Improved geophysical image of the Carpathian-Pannonian Basin region. Acta Geodaetica et Geophysica Hungarica, **45**, 3, 284–298.

Briestenský M., Košťák B., Stemberk J., Petro Ľ., Vozár J., Fojtíková L., 2010: Active tectonic fault microdisplacement analyses: a comparison of results from surface and underground monitoring in Western Slovakia. Acta Geodyn. Geomater., **7**, 4(160), 387–397.

Fojtíková L., Vavryčuk V., Cipciar A., Madarás J., 2010: Focal mechanisms of micro-earthquakes in the Dobrá Voda seismoactive area in the Malé Karpaty Mts (Little Carpathians), Slovakia. Tectonophysics, **492**, 213–229.

Galis M., Moczo P., Kristek J., 2008: A 3-D hybrid finite-difference—finite-element viscoelastic modeling of seismic wave motion. Geophys. J. Int., **175**, 153–184.

Galis M., Moczo P., Kristek J., Kristekova M., 2010: An adaptive smoothing algorithm in the TSN modelling of rupture propagation with the linear slip-weakening friction law. Geophys. J. Int., **180**, 418–432.

Grad M., Guterch A., Keller G. R., Brückl E., Belinsky A. A., Asudeh R. C., Hajnal Z., Špičák A., Jensen S. L., Thybo H., Komminaho K., Luosto U., Tiira T., Yliniemi J., Fancsik T., Hegedüs E., Kovacs A., Csabafi R., Jacyna J., Korabliova L., Motuza G., Nasedkin V., Czuba W., Gaczynski E., Janik T., Malinowski M., Slaczka A., Sroda P., Wilde-Piórko M., Kostiuchenko S. L., Bielik M., Vozár J., Selvi O., Harder S., Miller K. C., 2007: Variations in lithospheric structure across the margin of Baltica

in central Europe and role of the variscan and Carpathian orogenesis. Geological Society of America Memoir 200. In: 4-D framework of continental crust. Boulder, Geological Society of America, 341–356. ISBN 978-0-8137-1200-0.

Grinč M., Bielik M., Mojzeš A., Hók J., 2010: Results of the gravity field interpretation in the Turčianska Kotlina Basin. Contrib. Geophys. Geod., **40**, 2, 103–120.

Chaljub E., Moczo P., Tsuno S., Bard P.-Y., Kristek J., Käser M., Stupazzini M., Kristekova M., 2010: Quantitative Comparison of Four Numerical Predictions of 3D Ground Motion in the Grenoble Valley, France. Bull. Seism. Soc. Am., **100**, 1427–1455.

Kristek J., Moczo P., Galis M., 2009: A brief summary of some PML formulations and discretizations for the velocity-stress equation of seismic motion. Studia Geoph. Geod., **53**, 459–474.

Kristek J., Moczo P., Galis M., 2010: Stable discontinuous staggered grid in the finite-difference modeling of seismic motion. Geophys. J. Int., **183**, 1401–1407.

Kristekova M., Kristek J., Moczo P., 2009: Time-frequency misfit and goodness-of-fit criteria for quantitative comparison of time signals. Geophys. J. Int., **178**, 813–825.

Kristekova M., Moczo P., Labak P., Cipciar A., Fojtikova L., Madaras J., Kristek J., 2008: Time-Frequency Analysis of Explosions in the Ammunition Factory in Novaky, Slovakia. Bull. Seism. Soc. Am., **98**, 2507–2516.

Kytková B., Tomek Č., Bielik M., Putiš M., 2007: Interpretation of deep seismic reflection profiles in the northern part of the Malé Karpaty Mountains. Contrib. Geophys. Geod., **37**, 1, 43–58.

Moczo P., Kristek J., Galis M., Pazak P., 2010: On accuracy of the finite-difference and finite-element schemes with respect to P-wave to S-wave speed ratio. Geophys. J. Int., **182**, 493–510.

Moczo P., Kristek J., Galis M., Pazak P., Balazovjech M., 2007: The Finite-Difference and Finite-Element Modeling of Seismic Wave Propagation and Earthquake Motion. Acta Physica Slovaca, **57**, 177–406.

Moczo P., Robertsson J. O. A., Eisner L., 2007: The finite-difference time-domain method for modeling of seismic wave propagation. In Advances in Wave Propagation in Heterogeneous Earth, 421-516, R.-S. Wu and V. Maupin, eds., Advances in Geophysics, **48**, R. Dmowska, ed., Elsevier – Academic Press.

Plašienka D., Vozár J., Bielik M., 2008: The Pieniny Klippen Belt at the depth rooted, or unrooted? In: 6th Meeting of the Central European Tectonic Studies Group CETeG and 13th Meeting of the Czech Tectonic Studies Group ČTS. Upohlav, 23.-26.4.2008. SlovTec 08 Bratislava, Štátny geologický ústav D. Štúra, 104–108. ISBN 978-80-89343-01-0.

Radwan A. H., Bielik M., Dérerová J., Kohút I., Elsayed A. I., 2007: Determination of the lithospheric structure along a profile 1 in Aswan area: 2-D integrated geophysical modeling. Al-Azhar Bulletin of Science, **17**, 2, 23–33.

Skarlatoudis A. A., Papazachos C. B., Theodoulidis N., Kristek J., Moczo P., 2010: Local site-effects for the city of Thessaloniki (N. Greece) using a 3-D finite-difference method: a case of complex dependence on source and model parameters. Geophys. J. Int., **182**, 279–298.

Szalaiová E., Bielik M., Makarenko I., Legostaeva O., Hók J., Starostenko V., Šujan M., Šefara J., 2008: Calculation of a stripped gravity map with a high degree of accuracy: a case study of Liptovská Kotlina Basin (Northern Slovakia). Geological Quarterly, **52**, 2, 103–114.

Vozár J., Szalaiová V., Bielik M., Potfaj M., Grad M., Guterch A., Keller G. R., Janik T., Hegedüs E., Slaczka A., Tiira T., Yliniemi J., Vozár J., 2007: Transects across the geological units of the WesternCarpathians and interpretation (seismic, gravity, magnetoteluric). Mineralia Slovaca, **39**, 1, 25–26.